Chemosphere 171 (2017) 177–184

Contents lists available at ScienceDirect

Chemosphere

journal homepage: www.elsevier.com/locate/chemosphere

Development of dual-fluorescence cell-based biosensors for detecting the influence of environmental factors on nanoparticle toxicity

Junting Liang [a, b, c], Xuanyu Wang [a, c], Luzhi Li [a, c], Shengmin Xu [a, c], Jiang Jiang [d], Lijun Wu [a, c], Guoping Zhao [a, c, **], Shaopeng Chen [a, c, *]

[a] Key Laboratory of Ion Beam Bioengineering, Hefei Institutes of Physical Science, China Academy of Science, Hefei, Anhui, PR China
[b] School of Life Sciences, University of Science and Technology of China, Hefei, Anhui, PR China
[c] Key Laboratory of Environmental Toxicology and Pollution Control Technology of Anhui Province, Hefei, Anhui, PR China
[d] Department of Surgery-Transplant and Mary & Dick Holland Regenerative Medicine Program, University of Nebraska Medical Center, Omaha, NE 68198, United States

HIGHLIGHTS

- We created a novel dual-fluorescence biosensor system that exhibited good accuracy and high sensitivity via flow cytometric analysis.
- The toxicity of silver nanoparticles was evaluated by the biosensors and confirmed by conventional assays.
- The cell-based biosensors can potentially be applied to assess nanoparticle-toxicity risks.

ARTICLE INFO

Article history:
Received 14 September 2016
Received in revised form
9 December 2016
Accepted 16 December 2016
Available online 18 December 2016

Handling Editor: Tamara S. Galloway

Keywords:
Biosensor
Fluorescent protein
Nanoparticles
Environmental factor
Flow cytometry

ABSTRACT

With the expanding use of engineered nanoparticles (NPs), development of a high-throughput, sensitive method for evaluating NP safety is important. In this study, we developed cell-based biosensors to efficiently and conveniently monitor NP toxicity. The biosensor cells were obtained by transiently transfecting human cells with biosensor plasmids containing a *mCherry* gene regulated by an inducible promoter [an activator protein 1 (AP-1) promoter, an interleukin 8 (IL8) promoter, or a B cell translocation gene 2 (BTG2) promoter], with an enhanced green-fluorescent protein gene driven by the cytomegalovirus promoter as the internal control. After optimizing flow cytometric analysis, these dual-fluorescence cell-based biosensors were capable of accurately and rapidly detecting NP toxicity. We found that the responses of AP-1, BTG2, and IL8 biosensors in assessing the toxicity of silver nanoparticles (Ag NPs) showed good dose-related increases after exposure to Ag NPs and were consistent with data acquired by conventional assays, such as western blot, real-time polymerase chain reaction, and immunofluorescence. Further investigation of the effects of environmental factors on Ag NP toxicity revealed that aging in water, co-exposure with fulvic acid, and irradiation with ultraviolet A light could affect Ag NP-induced biosensor responses. These results indicated that these novel dual-fluorescence biosensors can be applied to accurately and sensitively monitor NP toxicity.

1. Introduction

The rapid development of nanotechnology promotes the wide application of engineered nanoparticles (NPs) in many fields, including industry, the pharmaceutical chemistry, and consumer goods (Emerich and Thanos, 2003; Mu and Sprando, 2010; Kaloyanova et al., 2016). Increasing types of novel NPs with special characteristics are constantly being synthesized (Piccinno et al., 2012). In the interests of biosecurity, health and environmental

* Corresponding author. Key Laboratory of Ion Beam Bioengineering, Hefei Institutes of Physical Science, Chinese Academy of Sciences, P. O. Box 1138, Hefei, Anhui 230031, PR China.
** Corresponding author. Key Laboratory of Ion Beam Bioengineering, Hefei Institutes of Physical Science, Chinese Academy of Sciences, P. O. Box 1138, Hefei, Anhui 230031, PR China.
E-mail addresses: gpz@ipp.ac.cn (G. Zhao), spchen035@ipp.ac.cn (S. Chen).

http://dx.doi.org/10.1016/j.chemosphere.2016.12.076
0045-6535/

risks should be assessed prior to NP application. Furthermore, engineered NPs are inevitably released into natural aquatic environments during the process of production and consumption. Environmental factors, such as ultraviolet A (UVA) irradiation, dissolved organic matter (DOM), pH, and ionic strength, can interact with nanoparticles, making the toxicity of transformed NPs in the environment a concern (El Badawy et al., 2010; Levard et al., 2012).

Some conventional analysis methods, including cell viability assays (AshaRani et al., 2009; Zhang et al., 2015, 2016a; Cheng et al., 2016), comet assays (Wang et al., 2014; Zhang et al., 2016b), and micronucleus testing (Li et al., 2012), are commonly applied to detect NP toxicity; however, these methods are elaborate and time-consuming (Karlsson et al., 2015). Additionally, NPs may interact with marker molecules or chemical agents, resulting in problems when conducting common toxicity tests (Kroll et al., 2012; Karlsson et al., 2013; Guadagnini et al., 2015). Investigation of apoptosis via AnnexinV/propidium-iodide staining has returned false-positive results in situations where NPs were able to bind propidium iodide and be taken up by intact cells (Darzynkiewicz et al., 2001; Shukla et al., 2005). NPs also interfere with enzyme-linked immunosorbent assays owing to the ability of NPs to adsorb cytokines (Monteiro-Riviere and Inman, 2006; Veranth et al., 2007).

The promoter-based biosensor system could be an alternative tool enabling the avoidance of interference and capable of performing high-throughput toxicity testing through acquisition of signals from reporter-gene expression. In these biosensors, the reporter gene is fused to a stress-responsive promoter, providing quantitative information in the form of a fluorescent signal when biosensor cells are exposed to conditions triggering a stress response. This method involving flow cytometric measurement is rapid and inexpensive as compared with conventional bioassays.

Cell-based biosensor systems have been employed to detect immunotoxicity (Oostingh et al., 2008; Stoehr et al., 2015), genotoxicity (Hever and Belkin, 2006; Geng et al., 2012; Blagus et al., 2014; Karlsson et al., 2014), and cell stress (Hofmann et al., 2014) induced by chemical compounds, with results comparable to those of conventional analysis methods [e.g., comet assays, immunocytochemistry, and real-time polymerase chain reaction (PCR)] (Oostingh et al., 2008; Hofmann et al., 2014; Karlsson et al., 2014). Some biosensor systems have been used to detect NP toxicity, based on responses triggering the activator protein 1 (AP-1) promoter (Prasad et al., 2013; Magaye, 2014), the interleukin 8 (IL8) promoter (Kohl, 2011; Stoehr et al., 2015), or the B cell translocation gene 2 (BTG2) promoter (Chen, 2012). AP-1 is a homodimer or heterodimer composed of the Jun, Fos, and activating transcription factor subgroups of transcription factors. Genes regulated by members of the AP-1 family are associated with proliferation, differentiation, cell death, and especially oncogenic transformation (Ding, 1999; Khanjani et al., 2012; Shaulian and Karin, 2001; Shaulian, 2002). IL8 is an important pro-inflammatory cytokine produced by different cell types in response to various stress stimuli. The 5′-flanking region of the IL8 gene contains a variety of potential binding sites for transcription factors, including nuclear factor kappa B, AP-1, and CAAT/enhancer-binding protein, along with the TATA box (Mukaida, 1994). BTG2 is a member of the BTG/TOB (B-cell translocation gene/transducers of ErbB2) gene family and acts as a DNA-damage marker used for detecting cytotoxicity involving DNA-strand breaks (Wada et al., 2009). The biosensor system is the basis for promising tools for toxicity assessment; however, current biosensors are normally limited by high background signals and internal-control deficiencies.

Here, to accurately and sensitively assess NP toxicity, we developed an improved dual-fluorescence biosensor system exhibiting reduced background signal and a validated internal control. Each biosensor plasmid was comprised of a *mCherry*-reporter gene regulated by an inducible promoter and an enhanced green-fluorescence protein (*EGFP*)-reporter gene driven by the cytomegalovirus (CMV) promoter as an internal control. AP-1, IL8, and BTG2 promoters were chosen as the inducible promoters. Using this dual-fluorescence biosensor system, we investigated the toxicity of silver NPs (Ag NPs) and the influence of environmental factors [aging, fulvic acid (FA), and UVA irradiation] on NP toxicity. Our results indicated that this novel cell-based biosensor system constituted an accurate and sensitive method for rapidly evaluating NP toxicity and exhibited great potential for applications involving the assessment of toxic risk.

2. Materials and methods

2.1. Cell lines and reagents

HeLa cells and 293T cells were grown in Dulbecco's modified Eagle medium (DMEM) containing 10% fetal bovine serum (FBS). Human non-small cell lung carcinoma H1299 cells were cultured in Roswell Park Memorial Institute 1640 medium supplemented with 10% FBS. Cells were maintained in a humidified atmosphere with 5% CO_2 at 37 °C. Ag NPs (polyvinylpyrrolidone-coated; <100 nm) and zinc oxide NPs were purchased from Sigma-Aldrich (St. Louis, MO, USA). Titanium dioxide NPs were purchased from NanoAmor (Houston, TX, USA). Lip2000 was purchased from Invitrogen (Carlsbad, CA, USA). Trizol and Power SYBR Green PCR master mix were purchased from Life Technologies, Inc. (Carlsbad, CA, USA), and TransScript One-Step gDNA removal and cDNA synthesis supermix was purchased from TransGen (Beijing, China).

2.2. Biosensor plasmid construction

The biosensor plasmid pAP1-MC-EGFP was constructed in four successive cloning steps. First, the *EGFP* fragment was subcloned into the Flag-CMV2 plasmid via *Hin*dIII and *Bam*HI restriction sites, using the forward primer 5′-TCGACT***AAGCTT***ATGGTGAG-CAAGGGCGAGGAG-3′ and the reverse prime 5′-TCACTG***GGATCC***T-TACTTGTACAGCTCGTCCATGCCG-3′ to yield pCMV-EGFP. The *mCherry* fragment was then digested with *Eco*RI and *Xba*I and introduced into the corresponding sites in the pcDNA3.1(+) plasmid to construct pcDNA-MC. Next, the AP-1 promoter was digested using *Bgl*II and *Kpn*I and inserted into pcDNA-MC upstream of the *mCherry* promoter to create pAP1-MC. Finally, the sequence containing the AP-1 consensus-binding sites and the *mCherry* gene was inserted into pCMV-EGFP by adding a *Bgl*II site to generate plasmid pAP1-MC-EGFP. The *CMV-EGFP* and *AP-1-mCherry* genes were designed to transcribe in opposite directions in the pAP1-MC-EGFP plasmid. An interference-blocking element consisting of two SV40 poly (A) sites was defined as transcription blocker (TB) and located upstream of the AP-1 promoter to prevent transcriptional interference of the downstream promoter.

The plasmids (pBTG2-MC-EGFP and pIL8-MC-EGFP) containing the BTG2 promoter (−110 bp to +71 bp) and the IL8 promoter (−179 bp to +69 bp) were constructed using a similar approach. Constructs were verified by sequencing.

2.3. Transfection for biosensor cells and nanoparticle exposure

Exponentially growing H1299 cells were seeded into 60-mm diameter Petri dishes (5×10^5 cells/dish) for 24 h. Transfection with empty plasmid or biosensor plasmid was performed using Lip2000 (Invitrogen) according to manufacturer instructions. After transfection, the cells were passaged into 12-well plates at 25,000 cells/well. Following overnight culture, the cells were

treated with Ag NPs (0, 5, 10, or 20 mg L^{-1}), and 24 h later, the cells were harvested and measured for promoter activity by flow cytometry. Before treatment, Ag NPs were dispersed in ultrapure water at the stock concentration of 1 mg mL^{-1}. Stock solutions were sonicated for 30 min and vortexed before taking aliquots to prepare working solutions (RPMI-1640 medium).

2.4. Flow cytometric analysis

Flow cytometric analysis for promoter activity was performed using a flow cytometer (BD Biosciences, San Jose, CA, USA). GFP fluorescence was used to indicate cells with transfected biosensor plasmids, and GFP-positive cells were gated for mCherry-fluorescence analysis. The percentage of mCherry-positive cells was analyzed with FACS Diva software (BD Biosciences). A total of 10,000 cells were collected per analysis, and data were expressed as the percentage of gated events. Promoter activity was calculated by dividing the percentage of mCherry-positive cells in NP-treated groups by that in untreated groups.

2.5. Western blot

After seeding and growing in the incubator, cells were treated with Ag NPs for 24 h. Following treatment, western blot was conducted as previously described (Xu et al., 2011). Expression of the c-Jun subunit of AP-1 was determined using an *anti-c*-Jun primary antibody (Cell Signaling Technology, Beverly, MA, USA). β-actin was used as an internal control.

2.6. Real-time PCR

Total RNA was isolated using Trizol reagent (Life Technologies, Inc.), and cDNA was generated using TransScript One-Step gDNA removal and cDNA synthesis supermix (TransGen) according to manufacturer protocol. Real-time PCR was performed in the ABI StepOne Plus real-time PCR system (Applied Biosystems, Foster City, CA, USA) using SYBR green detection as described previously (Wu et al., 2010). Relative gene expression was calculated according to the $\Delta\Delta Ct$ method, with β-actin used as a reference control.

2.7. Immunocytochemistry

γH2AX-foci formation assay was performed as previously described (Karlsson et al., 2014). Briefly, following treatment with 10 mg L^{-1} Ag NPs for 24 h, cells on glass slides were washed and fixed with 2% paraformaldehyde, then stained with γH2AX antibody (Novus Biological, Littleton, CO., USA) and Alexa488-labeled secondary antibody (Beyotime, Haimen, China). After staining the nucleus with 4′,6-diamidino-2-phenylindole (DAPI), cells were visualized by confocal microscopy (Carl Zeiss, Oberkochen, Germany).

2.8. Aging, UVA irradiation, and FA II treatment

To investigate the effect of natural aging on NP-induced promoter activity, aged Ag NPs were suspended in ultrapure water and stored at room temperature for the designated aging time. Irradiation experiments were performed using UV lamps with an emission-wavelength peak at 365 nm. The Ag NP suspension in culture media at the designated concentration was exposed to UVA irradiation, and the incident-light intensity was simultaneously measured using a radiometer (Photoelectric Instrument Factory of Beijing Normal University, Beijing, China). Suwannee River FA (FA standard II) was purchased from IHSS (St. Paul, MN, USA) and was investigated as a representative DOM. Upon exposure, the freshly prepared Ag NP suspension and FA were added into the cell culture media at the designated dosage and incubated for 24 h.

2.9. Statistical analysis

Data obtained from at least three independent experiments were expressed as the mean ± standard deviation and analyzed by one-way analysis of variance (ANOVA). Differences with a $p < 0.05$ were considered statistically significant.

3. Results

3.1. Design of a dual-fluorescence cell-based biosensor system

To monitor NP toxicity, biosensor plasmids (pAP1-MC-EGFP, pBTG2-MC-EGFP, and pIL8-MC-EGFP) were constructed (Fig. 1), with each plasmid consisting of two fluorescent-protein reporter genes, *EGFP* and *mCherry*. The expression of *mCherry* was under the control of an inducible promoter (IL8 promoter, BTG2 promoter, or AP-1 promoter), with *EGFP* driven by the CMV promoter as an internal control for quantitative analysis. The *EGFP* and *mCherry* sequences were designed to allow transcription in opposite directions to minimize the interference of gene expression. Use of the inducible promoters in the pIL8-MC-EGFP, pBTG2-MC-EGFP, and pAP1-MC-EGFP allowed activation by inflammatory response, DNA damage, or invasion potential, respectively.

3.2. Optimized flow cytometric analysis of biosensors

After transient transfection, cells were detected by flow cytometry. To enable accurate and sensitive analysis, the cells transfected with empty plasmid were used to set gates for EGFP-positive cells (P1; Fig. 2a and b). After the cells were transfected with biosensor plasmid, we found that some of the cells were outside of the P1 region, indicating that these cells failed to transfect or express EGFP protein. These cells were subsequently excluded from analysis, whereas those within the P1 region were

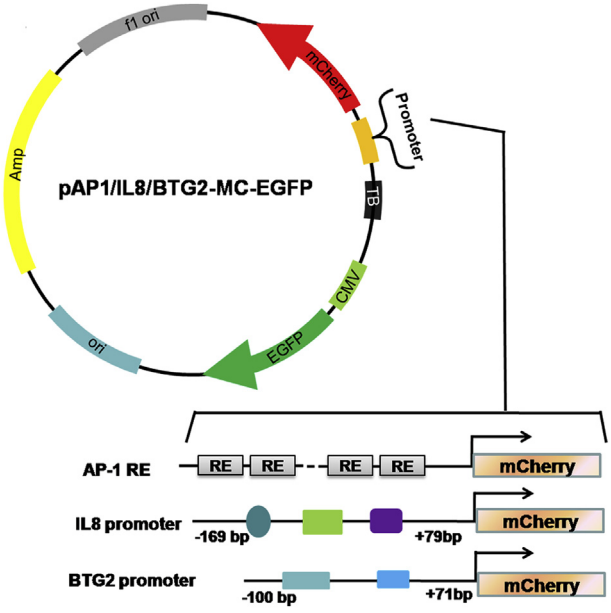

Fig. 1. Schematic representation of the dual-fluorescent biosensor system. AP-1 promoter, IL8 promoter, or BTG2 promoter was involved in the expression of *mCherry*, with EGFP fluorescence was acting as the internal control. TB was placed upstream of the inducible promoter to reduce background expression.

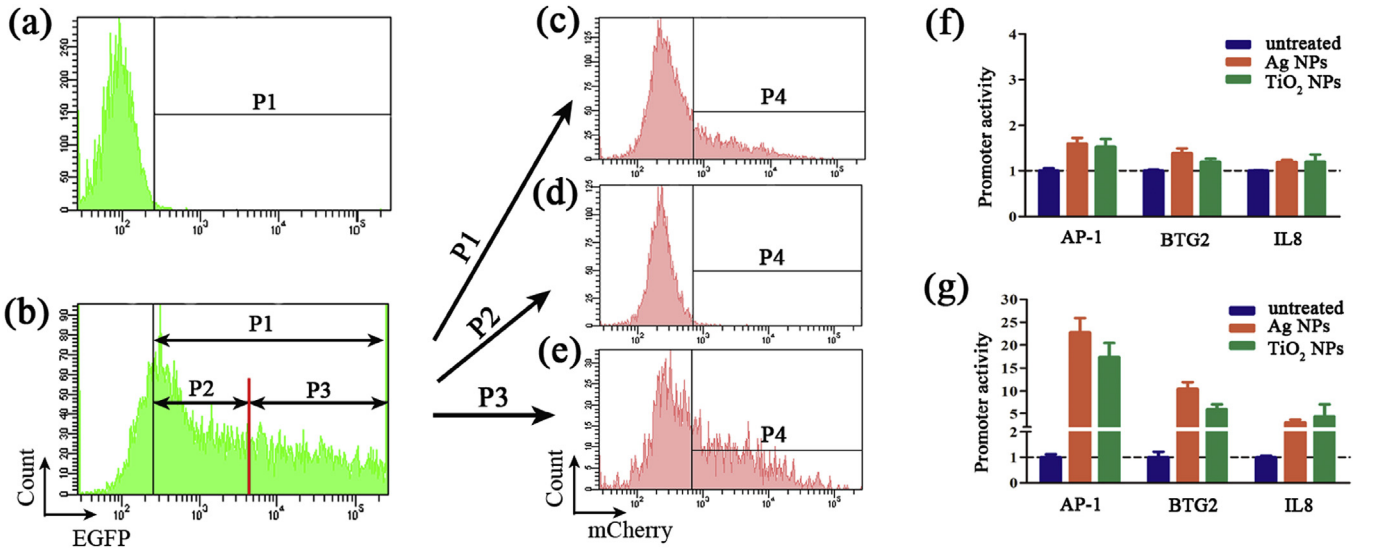

Fig. 2. Setting the gate of histogram to improve the sensitivity of dual-fluorescent biosensors using flow cytometry. Cells transfected with the biosensor plasmid were gated according to EGFP fluorescence in the EGFP histogram plots. The P1 region represented EGFP-positive cells (a, b). The mCherry fluorescence of the P1, P2, and P3 regions was analyzed, respectively. The percentage of the P4 region was acquired and represented promoter activity. The red line used to divide the P2 and P3 regions was established according to mCherry fluorescence in P4. When the background mCherry fluorescence in P4 was minimized, the red line was re-established. After treatment with nanoparticles for 24 h at 10 mg L^{-1}, the promoter activities of biosensor cells from the P1 and P2 regions were obtained. The biosensor cells in region P2 appeared more sensitive than those in region P1. Data are presented as mean x-fold increase over untreated controls. (For interpretation of the references to colour in this figure legend, the reader is referred to the web version of this article.)

analyzed to assess promoter activity. The percentage of mCherry-positive cells in the P1 region was acquired and analyzed in mCherry histogram plots (P4; Fig. 2c). However, EGFP-positive cells exhibited high background signals associated with mCherry, which decreased detection sensitivity. We then found that cells with lower levels of GFP fluorescence showed lower background mCherry fluorescence (Fig. 2d), and cells with higher levels of GFP fluorescence showed higher mCherry fluorescence (Fig. 2e), suggesting that cells expressing GFP at higher levels could induce promoter activity possibly related to stress induced by GFP overexpression.

To eliminate the effect of cells with high promoter activity and improve the sensitivity of the analysis, we dragged red line in Fig. 2b during flow cytometric analysis, and when the background mCherry fluorescence was minimized in Fig. 2d, the P2 were set. The right side of red line is P3 region. Following NP treatment, we detected and analyzed promoter activity in the P1 and P2 subpopulations (Fig. 2f and g). Fig. 2f showed that cells from the P1 region exhibited low detection sensitivity following NP treatment, whereas cells from the P2 region exhibited high detection sensitivity (Fig. 2g) after eliminating the interference of high-fluorescence signals as background. The cells in the P2 region were used as biosensor cells for detecting promoter activity in subsequent experiments. We also checked the effects of cell lines on promoter activity, finding that H1299 cells exhibited a higher response and lower background signal as compared with all tested cell lines (Fig. S1). Consequently, H1299 cells were used in all subsequent experiments to detect nanoparticle toxicity.

3.3. Relative sensitivity of biosensors

To determine the advantages associated with using dual-fluorescence biosensors, the sensitivity of pAP1-MC-EGFP established in this study was compared with that of the other two types of biosensors: 1) single-fluorescence biosensors using a single plasmid (pAP1-MC) without internal-control genes and 2) dual-color biosensors using two plasmids (pAP1-MC and pCMV-EGFP, containing a *mCherry* gene under the control of an inducible promoter and a constitutively expressed *EGFP* gene as an internal control, respectively). Three types of biosensor cells were obtained following transfection with pAP1-MC-EGFP, pAP1-MC, and pAP1-MC/pCMV-EGFP, and following NP treatment, we observed that the AP-1 response in pAP1-MC-EGFP biosensor cells was dramatically higher as compared with that observed in pAP1-MC cells or in pAP1-MC/pCMV-EGFP cells (Fig. 3). These results indicated that the dual-fluorescence biosensor associated with the pAP1-MC-EGFP plasmid was more sensitive and suitable for detecting nanoparticle cytotoxicity as compared with the other tested biosensors.

3.4. Ag NP induction of promoter activity

To explore the effects of NPs on promoter induction, biosensor cells were exposed to fresh Ag NPs for 24 h, followed by

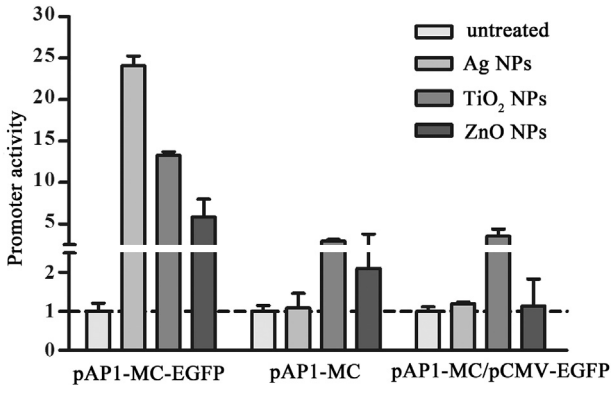

Fig. 3. Comparison of AP-1 activities in the cells transfected with pAP1-MC-EGFP, pAP1-MC and pAP1-MC plus pCMV-EGFP. Cells were transiently transfected with corresponding biosensor plasmids and exposed to nanoparticles at a concentration of 10 mg L^{-1} for 24 h. The induced AP-1 activities were measured by flow cytometry. Data are presented as mean x-fold increase over untreated control.

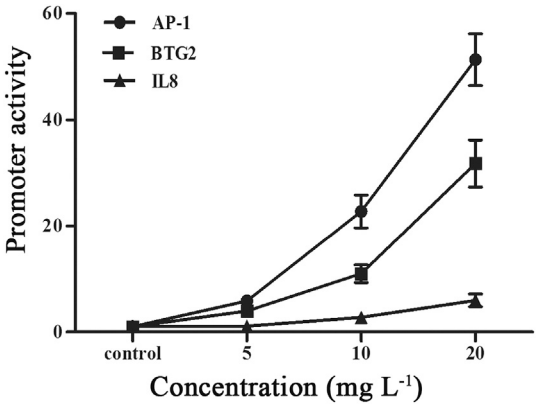

Fig. 4. Promoter activities induced by Ag NPs. Biosensor cells were treated with Ag NPs for 24 h, and promoter activities were measured by flow cytometry. Data are presented as mean x-fold increase over untreated control.

measurement of AP-1, BTG2, and IL8 transcriptional activity. Fig. 4 showed that Ag NP treatment increased the activities of the AP-1, BTG2, and IL8 promoters in a dose-dependent manner, with AP-1 activity increased by up to 5.9-, 22.8-, and 51.4-fold at NP concentrations of 5 mg L^{-1}, 10 mg L^{-1}, and 20 mg L^{-1}, respectively (Fig. 4). Similarly, transcription of the BTG2 promoter was significantly enhanced by ~4.0-, 11.0-, and 31.8-fold, and IL8 transcription was enhanced by 1.5-, 2.8-, and 6.0-fold at NP concentrations of 5 mg L^{-1}, 10 mg L^{-1}, and 20 mg L^{-1}, respectively. These results suggested that Ag NP exposure induced dose-dependent activities of inducible promoters that were related to inflammatory response, DNA damage, and potential carcinogenesis.

3.5. Confirmation of Ag NP-induced promoter response using conventional assays

To confirm promoter response, we assessed biosensor-cell response to Ag NP treatment in H1299 cells using conventional assays. Western blot revealed significantly higher levels of the c-Jun subunit of AP-1 induced by Ag NP as compared with levels observed in untreated groups (Fig. 5a). To compare this result with IL8-promoter activity, we determined the expression level of IL8 mRNA by real-time PCR. In Ag NP-treated cells, IL8 mRNA was clearly induced (Fig. 5b). Moreover, DNA double-strand breaks were detected by a γH2AX-formation assay. In this assay, the histone variant H2AX is rapidly phosphorylated at double-strand breaks in DNA, subsequently generating γH2AX as a product (Ivashkevich et al., 2012). Exposure of the cells to Ag NPs led to an increase in γH2AX-foci formation (Fig. 5c and d). These data from conventional assays were consistent with results from the dual-fluorescence biosensor assay, suggesting that these cell-based biosensors are promising and alternative tools for the assessment of NP risk.

3.6. Influence of environmental factors on Ag NP-induced promoter activity

NPs age in the environment, making it is necessary to detect the toxicity of aged NPs. To investigate the aging processes associated with different NPs and their effect on biosensor transcriptional activity, Ag NPs were suspended in ultrapure water for the

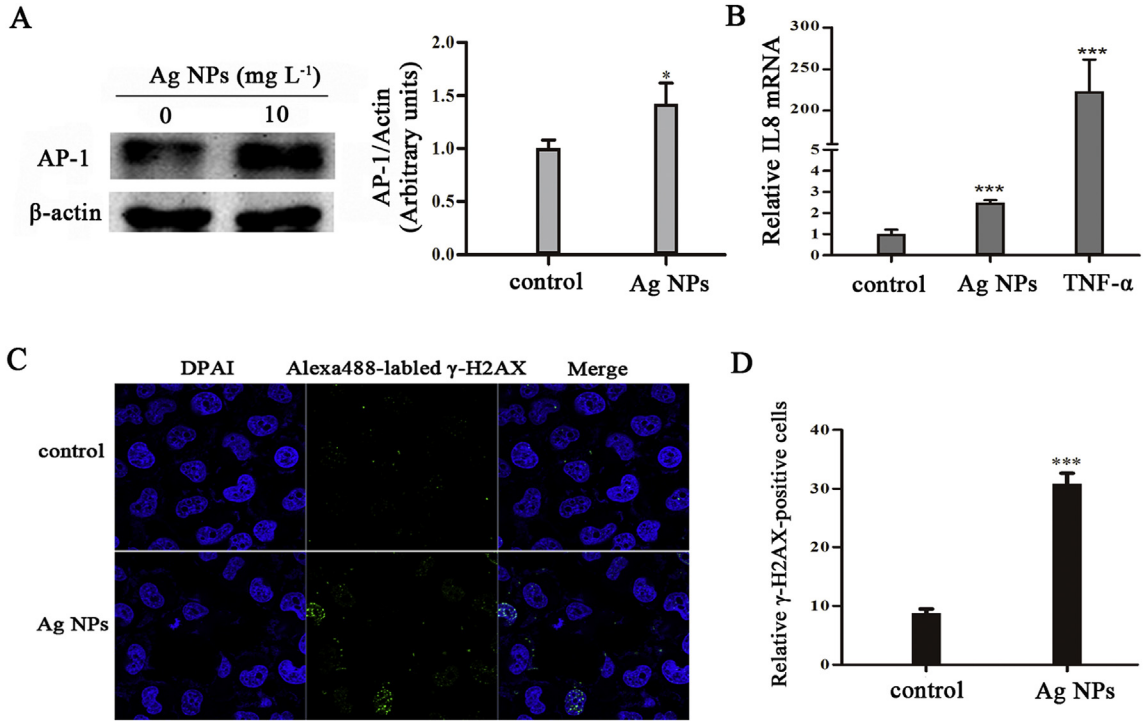

Fig. 5. Conventional assays confirmed the biosensor response of the biosensors. H1299 cells were treated with Ag NPs for 24 h at 10 mg L^{-1}, and cells were tested for the assays as follows: (a) effects of Ag NPs on protein expression of the c-Jun subunit of AP-1 as measured by western blot, with β-actin as an internal control and band density measured by ImageJ software and normalized to that of β-actin (AP-1 levels in treated cells were expressed as arbitrary units relative to controls); (b) IL8 mRNA levels determined by reverse transcription PCR, using TNF-α as a positive control; (c) representative images of γH2AX foci. Fixed cells were labeled with γH2AX primary antibody and stained with Alexa488-labeled secondary antibody (green). DAPI was used to visualize the nucleus in blue. (d) Incidence of γH2AX foci in Ag NP-treated cells. Counting values represented a percentage of γH2AX-positive cells. Data were analyzed with one-way ANOVA. $^{*}p < 0.05$; $^{***}p < 0.01$. (For interpretation of the references to colour in this figure legend, the reader is referred to the web version of this article.)

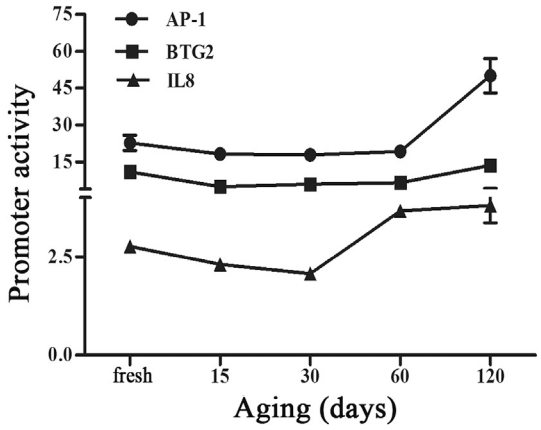

Fig. 6. Promoter activities induced by aged Ag NPs. Biosensor cells were treated with aged Ag NPs at 10 mg L^{-1} for 24 h, followed by measurement of promoter activities by flow cytometry. Data are presented as mean x-fold increase over untreated control.

designated times prior to exposure. Ag NPs aged 120 days induced higher AP-1-promoter activity, and Ag NPs aged 60 or 120 days induced higher IL8-promoter activity as compared with activity induced by fresh Ag NPs (Fig. 6). Interestingly, BTG2-promoter activity induced by Ag NPs aged for 15, 30, or 60 days (4.9-, 6.0-, or 6.6-fold, respectively) was significantly lower than that induced by fresh Ag NPs (11.0-fold). BTG2 levels exposed to Ag NPs aged for 120 days increased to levels (13.6-fold) similar to those observed following exposure to fresh Ag NPs. These data indicated that aging dramatically altered Ag NP toxicity.

Exposure of NPs to sunlight was simulated by UVA irradiation (Tu et al., 2012). To further investigate the role of UVA irradiation on NP toxicity, Ag NPs were irradiated by UVA at graded doses ranging from 0.28 J/cm^2 to 1.26 J/cm^2, followed by exposure of biosensor cells to UVA-treated Ag NPs to examine promoter activity. As shown in Table 1, UVA-irradiated Ag NPs induced lower transcriptional activity in all promoters (AP-1, IL8, and BTG2) as compared with non-irradiated Ag NPs. These results indicated that UVA-irradiated Ag NPs induced less toxic effects relative to non-irradiated controls.

To assess the influence of DOM, promoter activities were measured in the presence of FA, which was used as a model for DOM. The dose of FA used in this study had no effect on promoter activities (data not shown) of the biosensors. As shown in Table 1, the activities of all three promoters decreased following co-exposure to Ag NPs and FA (Table 1). Therefore, administration of FA decreased Ag NP toxicity.

4. Discussion

The production and use of engineered NPs call for rapid, reliable, and high-throughput toxicity testing to facilitate understanding of the mechanisms associated with NP toxicity and improve NP biocompatibility. Cell-based biosensor systems are promising analytical tools for assessing the health and environmental risks of NPs. There are currently two types of toxicity biosensors. One involves a plasmid containing an inducible promoter that controls a reporter gene. Optimal results would be generated with regard to high-efficient transfection of single-biosensor plasmids or construction of time-consuming stable cell lines (Legler et al., 2002; Novotna et al., 2011). The other type of biosensor uses two plasmids, including one containing a constitutively expressed reporter gene as an internal control to standardize transfection efficiency and a biosensor plasmid containing an inducible promoter and a reporter gene. However, the internal control in two-plasmid-based biosensors is often inaccurate owing to variations in the efficiency of plasmid co-transfection (Asea et al., 2002). Here, we developed a novel dual-fluorescence biosensor system using AP-1, BTG2, or IL8 promoters to measure NP toxicity. We combined constitutive (*EGFP*) and inducible (*mCherry*) reporter genes into one biosensor plasmid, enabling accurate control of normalized transfections. With EGFP as an internal control, biosensor cells can be differentiated and gated by EGFP fluorescence, and the experiments can be performed with transient transfections instead of time-consuming stable transfections. Furthermore, we optimized flow cytometric analysis by resetting the gates of EGFP-positive cells to eliminate the interference of background signals (Fig. 2). These innovations allowed us to significantly improve the sensitivity of the developed biosensors.

Multiple biological endpoints are necessary to accurately analyze toxic effects. Previous studies reported cell-based biosensors working together with traditional methods to perform toxicity assessment (Wu et al., 2010; Blagus et al., 2014; Stoehr et al., 2015). Here, exposure of biosensor cells to Ag NPs induced the response of the AP-1, BTG2, and IL8 reporters, indicating that Ag NP toxicity was involved in potential carcinogenesis, DNA damage, or inflammatory response. This response was in agreement with tests using conventional assays, including western blot (AP-1 expression), real-time PCR (IL8 mRNA levels), and immunocytochemistry assays (γH2AX-foci formation) (Fig. 5). Compared with traditional toxicity testing, combining biosensors provides advantages, including simplified assay procedures, cost-efficient methods, and the kinetics of gene expression, to exhibit excellent performance of high-throughput toxicity testing (Blagus et al., 2014; Hofmann et al., 2014; Karlsson et al., 2014).

During production and consumption, NPs are inevitably released into the natural aquatic environment and will continuously interact with complex environmental factors, resulting in variations in NP biotoxicity. Previous studies showed that aged Ag NPs are more toxic to cells as compared with freshly prepared Ag NPs (Kittler et al., 2010). This finding agreed with our results from dual-fluorescence biosensor assays. Reduced surface charge could

Table 1
Promoter activities induced by UVA-irradiated Ag NPs or co-exposed to Ag NPs and FA. Ag NPs were used at 10 mg L^{-1}. Values were presented as mean x-fold increase over untreated control and data were analyzed with one-way ANOVA (*p-value <0.05, **p-value <0.01 versus groups treated only by Ag NPs).

Particles	Environmental factor	Dose	Fold of induced promoter activities		
			AP-1	BTG2	IL8
Ag NPs 10 mg L^{-1}	UVA (J/cm^2)	0	23 ± 3.1	11 ± 1.7	2.8 ± 0.1
		0.28	7.8 ± 0.4**	6.4 ± 0.8*	1.6 ± 0.2**
		0.56	9.4 ± 1.4**	9.9 ± 1.4	1.3 ± 0.3**
		0.84	12 ± 2.1**	5.3 ± 0.3**	1.2 ± 0.4**
		1.26	13 ± 2.6*	4.7 ± 0.5**	1.5 ± 0.1**
	FA (mg L^{-1})	10	9.4 ± 1.7**	6.3 ± 1.7**	1.8 ± 0.1**
		20	9.5 ± 1.3**	6.2 ± 0.9**	1.5 ± 0.1**

also promote the aging process and contribute to the cytotoxicity conferred by exposure to aged Ag NPs (Table S1). Additionally, Ag NP toxicity was reduced following exposure to simulated sunlight irradiation, which is a driving force in NP aggregation (Cheng et al., 2011). Similarly, we observed that Ag NPs irradiated with UVA showed reduced toxicity relative to DNA damage, immune-response activity, and carcinogenic hazard. Furthermore, FA administration also reduced Ag NP toxicity. The underlying mechanisms associated with this reduction may involve FA adsorption onto Ag NPs acting as a physical barrier to reduce the interactions between cells and NPs (Domingos et al., 2009). Furthermore, an NP-protein corona is formed on the surface of particles upon their exposure to biological media. Therefore, FA might also participate in the formation of protein coronas that affect Ag NP stability (Delay et al., 2011). Ag NP toxicity was lower in the presence of FA in biological media, mostly resulting from the indirect contact between NPs and cells (Fabrega et al., 2009).

5. Conclusion

In summary, this study developed a novel dual-fluorescence biosensor system based on three inducible promoters (AP-1 promoter, IL8 promoter, or BTG2 promoter). By optimizing flow cytometric analysis, the accuracy and sensitivity of these biosensors were improved. Using these biosensors, the toxicity of nanoparticles was detected rapidly and sensitively, and the results were consistent with those of conventional assays. These designed biosensors provide a rapid and sensitive method for assessing nanoparticle toxicity.

Acknowledgements

This work was supported by grants from Major National Scientific Research Projects, 2014CB932002; Strategic Leading Science & Technology Program (B), XDB14030502; CASHIPS director's fund, YZJJ201501; The Major/Innovative Program of Development Foundation of Hefei Center for Physical Science and Technology, 2014FXCX010; CAS Pioneer Hundred Talents Program (GZ); The CAS/SAFEA International Partnership Program for Creative Research Teams; The China Postdoctorial Science Foundation, 2016M602044.

Appendix A. Supplementary data

Supplementary data related to this article can be found at http://dx.doi.org/10.1016/j.chemosphere.2016.12.076.

References

Asea, A., Rehli, M., Kabingu, E., Boch, J.A., Bare, O., Auron, P.E., Stevenson, M.A., Calderwood, S.K., 2002. Novel signal transduction pathway utilized by extracellular HSP70-Role of Toll-like receptor (TLR) 2 AND TLR4. J. Biol. Chem. 277, 15028–15034.
AshaRani, P.V., Low Kah, M.G., Hande, M.P., Valiyaveettil, S., 2009. Cytotoxicity and genotoxicity of silver nanoparticles in human cells. ACS Nano 3.
Blagus, T., Zager, V., Cemazar, M., Sersa, G., Kamensek, U., Zegura, B., Nunic, J., Filipic, M., 2014. A cell-based biosensor system HepG2CDKN1A-DsRed for rapid and simple detection of genotoxic agents. Biosens. Bioelectron. 61, 102–111.
Chen, P., 2012. Detection of DNA damage response caused by different forms of titanium dioxide nanoparticles using sensor cells. J. Biosens. Bioelectron. 03.
Cheng, Y.W., Yin, L.Y., Lin, S.H., Wiesner, M., Bernhardt, E., Liu, J., 2011. Toxicity reduction of polymer-stabilized silver nanoparticles by sunlight. J. Phys. Chem. C 115, 4425–4432.
Cheng, Y.Y., Li, G.C., Liu, Y., Shi, Y., Gao, G., Wu, D., Lan, J.B., You, J.S., 2016. Unparalleled ease of access to a library of biheteroaryl fluorophores via oxidative cross-coupling reactions: discovery of photostable NIR probe for mitochondria. J. Am. Chem. Soc. 138, 4730–4738.
Darzynkiewicz, Z., Bedner, E., Traganos, F., 2001. Difficulties and pitfalls in analysis of apoptosis. Methods Cell Biol. 63, 527–546.
Delay, M., Dolt, T., Woellhaf, A., Sembritzki, R., Frimmel, F.H., 2011. Interactions and stability of silver nanoparticles in the aqueous phase: influence of natural organic matter (NOM) and ionic strength. J. Chromatogr. A 1218, 4206–4212.
Ding, M., 1999. Freshly fractured crystalline silica induces activator protein-1 activation through ERKs and p38 MAPK. J. Biol. Chem. 274, 30611–30616.
Domingos, R.F., Tufenkji, N., Wilkinson, K.I., 2009. Aggregation of titanium dioxide nanoparticles: role of a fulvic acid. Environ. Sci. Technol. 43, 1282–1286.
El Badawy, A.M., Luxton, T.P., Silva, R.G., Scheckel, K.G., Suidan, M.T., Tolaymat, T.M., 2010. Impact of environmental conditions (pH, ionic strength, and electrolyte type) on the surface charge and aggregation of silver nanoparticles suspensions. Environ. Sci. Technol. 44, 1260–1266.
Emerich, D.F., Thanos, C.G., 2003. Nanotechnology and medicine. Expert Opin. Biol. Ther. 3, 655–663.
Fabrega, J., Fawcett, S.R., Renshaw, J.C., Lead, J.R., 2009. Silver nanoparticle impact on bacterial growth: effect of pH, concentration, and organic matter. Environ. Sci. Technol. 43, 7285–7290.
Geng, D., Zhang, Z., Guo, H., 2012. Development of a fish cell biosensor system for genotoxicity detection based on DNA damage-induced trans-activation of p21 gene expression. Biosensors 2, 318–340.
Guadagnini, R., Kenzaoui, B.H., Walker, L., Pojana, G., Magdolenova, Z., Bilanicova, D., Saunders, M., Juillerat-Jeanneret, L., Marcomini, A., Huk, A., Dusinska, M., Fjellsbo, L.M., Marano, F., Boland, S., 2015. Toxicity screenings of nanomaterials: challenges due to interference with assay processes and components of classic in vitro tests. Nanotoxicology 9, 13–24.
Hever, N., Belkin, S., 2006. A dual-color bacterial reporter strain for the detection of toxic and genotoxic effects. Eng. Life Sci. 6, 319–323.
Hofmann, U., Priem, M., Bartzsch, C., Winckler, T., Feller, K.H., 2014. A sensitive sensor cell line for the detection of oxidative stress responses in cultured human keratinocytes. Sensors 14, 11293–11307.
Ivashkevich, A., Redon, C.E., Nakamura, A.J., Martin, R.F., Martin, O.A., 2012. Use of the gamma-H2AX assay to monitor DNA damage and repair in cancer research. Cancer Lett. 327, 123–133.
Kaloyanova, S., Zagranyarski, Y., Ritz, S., Hanulova, M., Koynov, K., Vonderheit, A., Mullen, K., Peneva, K., 2016. Water-soluble NIR-absorbing rylene chromophores for selective staining of cellular organelles. J. Am. Chem. Soc. 138, 2881–2884.
Karlsson, H.L., Cronholm, P., Hedberg, Y., Tornberg, M., De Battice, L., Svedhem, S., Wallirider, I.O., 2013. Cell membrane damage and protein interaction induced by copper containing nanoparticles-Importance of the metal release process. Toxicology 313, 59–69.
Karlsson, H.L., Di Bucchianico, S., Collins, A.R., Dusinska, M., 2015. Can the comet assay be used reliably to detect nanoparticle-induced genotoxicity? Environ. Mol. Mutagen. 56, 82–96.
Karlsson, H.L., Gliga, A.R., Calleja, F.M., Goncalves, C.S., Wallinder, I.O., Vrieling, H., Fadeel, B., Hendriks, G., 2014. Mechanism-based genotoxicity screening of metal oxide nanoparticles using the ToxTracker panel of reporter cell lines. Part Fibre Toxicol. 11, 41.
Khanjani, S., Terzidou, V., Johnson, M.R., Bennett, P.R., 2012. NFkappaB and AP-1 drive human myometrial IL8 expression. Mediat. Inflamm. 2012, 504952.
Kittler, S., Greulich, C., Diendorf, J., Koller, M., Epple, M., 2010. Toxicity of silver nanoparticles increases during storage because of slow dissolution under release of silver Ions. Chem. Mater. 22, 4548–4554.
Kohl, Y., 2011. Biocompatible micro-sized cell culture chamber for the detection of nanoparticle-induced IL8 promoter activity on a small cell population. Nanoscale Res. Lett. 6, 505.
Kroll, A., Pillukat, M.H., Hahn, D., Schnekenburger, J., 2012. Interference of engineered nanoparticles with in vitro toxicity assays. Arch. Toxicol. 86, 1123–1136.
Legler, J., Zeinstra, L.M., Schuitemaker, F., Lanser, P.H., Bogerd, J., Brouwer, A., Vethaak, A.D., De Voogt, P., Murk, A.J., Van der Burg, B., 2002. Comparison of in vivo and in vitro reporter gene assays for short-term screening of estrogenic activity. Environ. Sci. Technol. 36, 4410–4415.
Levard, C., Hotze, E.M., Lowry, G.V., Brown Jr., G.E., 2012. Environmental transformations of silver nanoparticles: impact on stability and toxicity. Environ. Sci. Technol. 46, 6900–6914.
Li, Y., Chen, D.H., Yan, J., Chen, Y., Mittelstaedt, R.A., Zhang, Y., Biris, A.S., Heflich, R.H., Chen, T., 2012. Genotoxicity of silver nanoparticles evaluated using the Ames test and in vitro micronucleus assay. Mutat. Research/Genetic Toxicol. Environ. Mutagen. 745, 4–10.
Magaye, R., 2014. Metallic nickel nanoparticles may exhibit higher carcinogenic potential than fine particles in JB6 cells. PloS One 9.
Monteiro-Riviere, N.A., Inman, A.O., 2006. Challenges for assessing carbon nanomaterial toxicity to the skin. Carbon 44, 1070–1078.
Mu, L., Sprando, R.L., 2010. Application of nanotechnology in cosmetics. Pharm. Res. 27, 1746–1749.
Mukaida, N., 1994. Molecular mechanism of interleukin-8 gene expression. J. Leokocyte Biol. 56.
Novotna, A., Petr, P., Dvorak, Z., 2011. Novel Stably transfected gene reporter human hepatoma cell line for assessment of aryl hydrocarbon receptor transcriptional activity: construction and characterization. Environ. Sci. Technol. 45, 10133–10139.
Oostingh, G.J., Schmittner, M., Ehart, A.K., Tischler, U., Duschl, A., 2008. A high-throughput screening method based on stably transformed human cells was used to determine the immunotoxic effects of fluoranthene and other PAHs. Toxicol. In Vitro Int. J. Publ. Assoc. BIBRA 22, 1301–1310.
Piccinno, F., Gottschalk, F., Seeger, S., Nowack, B., 2012. Industrial production quantities and uses of ten engineered nanomaterials in Europe and the world. J. Nanoparticle Res. 14.

Prasad, R.Y., McGee, J.K., Killius, M.G., Suarez, D.A., Blackman, C.F., DeMarini, D.M., Simmons, S.O., 2013. Investigating oxidative stress and inflammatory responses elicited by silver nanoparticles using high-throughput reporter genes in HepG2 cells: effect of size, surface coating, and intracellular uptake. Toxicol. In Vitro Int. J. Publ. Assoc. BIBRA 27, 2013–2021.

Shaulian, E., 2002. AP-1 as a regulator of cell life and death. Nat. Cell Biol. 4.

Shaulian, E., Karin, M., 2001. AP-1 in cell proliferation and survival. Oncogene 20, 2390–2400.

Shukla, S., Priscilla, A., Banerjee, M., Bhonde, R.R., Ghatak, J., Satyam, P.V., Sastry, M., 2005. Porous gold nanospheres by controlled transmetalation reaction: a novel material for application in cell imaging. Chem. Mater. 17, 5000–5005.

Stoehr, L.C., Endes, C., Radauer-Preiml, I., Boyles, M.S., Casals, E., Balog, S., Pesch, M., Petri-Fink, A., Rothen-Rutishauser, B., Himly, M., Clift, M.J., Duschl, A., 2015. Assessment of a panel of interleukin-8 reporter lung epithelial cell lines to monitor the pro-inflammatory response following zinc oxide nanoparticle exposure under different cell culture conditions. Part Fibre Toxicol. 12, 29.

Tu, M., Huang, Y., Li, H.L., Gao, Z.H., 2012. The stress caused by nitrite with titanium dioxide nanoparticles under UVA irradiation in human keratinocyte cell. Toxicology 299, 60–68.

Veranth, J.M., Kaser, E.G., Veranth, M.M., Koch, M., Yost, G.S., 2007. Cytokine responses of human lung cells (BEAS-2B) treated with micron-sized and nanoparticles of metal oxides compared to soil dusts. Part Fibre Toxicol. 4, 2.

Wada, K.-I., Hamaguchi, Y., Furukawa, K., Taniguchi, A., 2009. DNA damage sensible engineered promoter for cellular biosensing of cytotoxicity. Biotechnol. Bioeng. 102, 1460–1465.

Wang, Y., Cui, H., Zhou, J., Li, F., Wang, J., Chen, M., Liu, Q., 2014. Cytotoxicity, DNA damage, and apoptosis induced by titanium dioxide nanoparticles in human non-small cell lung cancer A549 cells. Environ. Sci. Pollut. Res. 22, 5519–5530.

Wu, W.D., Samet, J.M., Peden, D.B., Bromberg, P.A., 2010. Phosphorylation of p65 is required for zinc oxide nanoparticle-induced interleukin 8 expression in human bronchial epithelial cells. Environ. Health Perspect. 118, 982–987.

Xu, Z., Ren, T., Xiao, C., Li, H., Wu, T., 2011. Nickel promotes the invasive potential of human lung cancer cells via TLR4/MyD88 signaling. Toxicology 285, 25–30.

Zhang, H., Wang, C., Jiang, T., Guo, H., Wang, G., Cai, X., Yang, L., Zhang, Y., Yu, H., Wang, H., Jiang, K., 2015. Microtubule-targetable fluorescent probe: site-specific detection and super-resolution imaging of ultratrace tubulin in microtubules of living cancer cells. Anal. Chem. 87, 5216–5222.

Zhang, H., Wang, C., Wang, K., Xuan, X., Lv, Q., Jiang, K., 2016a. Ultrasensitive fluorescent ratio imaging probe for the detection of glutathione ultratrace change in mitochondria of cancer cells. Biosens. Bioelectron. 85, 96–102.

Zhang, H., Wang, K., Xuan, X.P., Lv, Q.Z., Nie, Y.M., Guo, H.M., 2016b. Cancer cell-targeted two-photon fluorescence probe for the real-time ratiometric imaging of DNA damage. Chem. Commun. 52, 6308–6311.